RSC Advances

ROYAL SOCIETY OF CHEMISTRY

www.rsc.org/advances

Cite this: DOI: 10.1039/c0xx00000x

www.rsc.org/xxxxxx

ARTICLE TYPE

Mesostructured Pd/Mn_3O_4 Catalyst for Efficient Low-temperature CO Oxidation Especially under Moisture Condition

Gengnan Li,[a] Liang Li,*[a] Yuan Yuan,[a] Yinyin Yuan,[a] Yongsheng Li,[a] Wenru Zhao[a] and Jianlin Shi*[a,b]

Received (in XXX, XXX) Xth XXXXXXXXX 20XX, Accepted Xth XXXXXXXXX 20XX

DOI: 10.1039/b000000x

Mesostructured Mn_3O_4 supported Pd catalyst was successfully fabricated through a facile template-assisted pyrolysis and impregnation strategy. The resulting materials displayed large surface area and high dispersion of palladium species, and showed much enhanced catalytic activities for CO oxidation especially under moisture atmosphere. For 2.7 wt% Pd loaded catalyst, the temperatures for 100 % and 50 % CO conversions were measured to be as low as 22 °C and 0 °C (4.0 vol% H_2O), respectively. More importantly, the material showed excellent catalytic stability and no activity loss was found even after the reaction for 30 hours. This unique catalytic durability under moisture condition was assigned to the synergetic effect between Pd nanoparticles and Mn_3O_4 support.

Introduction

Over the past decade, the development of low temperature carbon monoxide oxidation catalyst has become an important research topic due to its wide applications in energy and environmental fields, such as hydrogen purification for proton exchange membrane fuel cell, automobile emissions controlling, CO gas detecting, and indoor air cleaning, et al. [1-6] The fundamental research about CO oxidation so far is usually under dry condition. However, moisture inevitably exists in practical use especially for that at low temperature, and plays completely different role in the presence/absence of noble metals in CO oxidation process. It could be a devastatingly poisonous species for transition metal oxides or a promoter for noble metal catalysts, which are two common types of catalyst for CO oxidation. [7-10] Thus, it is more important to study the catalytic behaviour of CO oxidation under moisture condition. Up to now, although there are some reports about highly active Au loaded catalyst which showed much higher water residence at low temperature, [11, 12] it still has some unsolved deficiencies, such as deactivation in storage and under indoor light, sensitiveness to halogen-including compound et al. [13-16] The catalyst for low temperature CO oxidation under moisture condition is still expected and in challenge.

Compared with Au catalyst, palladium has much stronger anti-poison properties, and is also promising catalyst for CO oxidation, especially for that supported on charge-variable transition metal oxides. [17-24] Benefited from the various oxidation states, charge-variable transition metal oxides possess excellent performance in oxygen storage and release which are also critical factors for low temperature CO oxidation. When combined with Pd nanoparticles, significantly enhanced activity could be achieved. Mn_3O_4 contains two relatively low oxidation state manganese ions, which not only benefit electron transferring, but also possess much higher oxygen storage and release capacity. It is therefore expected that mesoporous Mn_3O_4 supported Pd catalyst should give the excellent catalyst for CO oxidation under moisture condition.

In this paper, mesoporous Mn_3O_4 material was prepared by template-assisted pyrolysis method, and Pd nanoparticles were confined within the mesostructure of Mn_3O_4 matrix through improved impregnation and in-situ reduction strategy. The catalytic activities and water resistance for the resulting Pd/Mn_3O_4 materials were investigated by CO oxidation reaction under different reaction conditions. The CO oxidation mechanism upon Pd/Mn_3O_4 catalyst was also discussed in detail.

Experimental section

Synthesis of mesoporous Mn_3O_4

1.0 g poly(ethylene glycol)-poly(propylene glycol)-poly(ethylene glycol) (P123) and 0.01 M $Mn(NO_3)_2$ was successively added to 10 ml anhydrous ethanol under vigorously stirring for 60 min. Then the mixture was transferred to an oven for complete solvent evaporation at 60 °C for 48 h. The resulting xerogel was calcined at 500 °C for 1 h to remove the template.

Synthesis of supported Pd/Mn_3O_4 catalysts

A series of mesoporous Mn_3O_4 supported Pd catalysts were synthesized through impregnation and reduction procedure. In a typical synthesis, 0.5 g mesoporous Mn_3O_4 material was added in 25 ml aqueous solution containing calculated content of Na_2PdCl_4 and stirred for 2 h. Then 100 ml 0.1 M hydrazine hydrate ($NH_2{\cdot}NH_2{\cdot}H_2O$) was added and stirred for 12 h. The resulting solid mass was collected through centrifugation, washed with

water and dried at 60 °C for 24 h.

CO oxidation test

The catalytic test for CO oxidation was carried out in fixed-bed quartz tubular reactor (i.d. = 6 mm) containing 200 mg of catalyst samples without any pre-treatment. A standard reaction gas containing 1.0 vol% CO, 20.0 vol% O_2 and high-purity N_2 (99.99%) gas used as sources to form desired gas mixture. The feed gas at a flow rate of 50 ml min^{-1} was introduced into the reactor using mass-flow controllers, corresponding to a space velocity of 15000 ml h^{-1} g_{cat}^{-1}. After the steady operation for 10 min, the activity of catalyst was tested. The conversion of CO was measured by online gas chromatograph (GC) equipped with a FID under steady-state conditions. The composition of the influent and effluent gas was first separated by a TDX-01 column. Then, the CO and CO_2 gas were catalytically converted to CH_4 by a Ni catalyst prior to the FID measurement. The reaction temperature was monitored by a thermocouple placed in the middle of the catalyst bed. The activity of the catalyst in the presence of moisture condition was tested by passing the feed gas of 1.0 vol% CO at a flow rate of 50 ml min^{-1} through a water vapor saturator directly introduced into the catalyst bed.

Results and discussion

The actual contents of Pd in the mesostructured Pd/Mn_3O_4 materials were determined by the ICP-AES technique to be 1.1, 2.7 and 3.2 wt%. Although the Pd loading contents were somewhat lower than the initial values, most of the Pd in the aqueous solution have been deposited into or on the mesoporous Mn_3O_4 support.

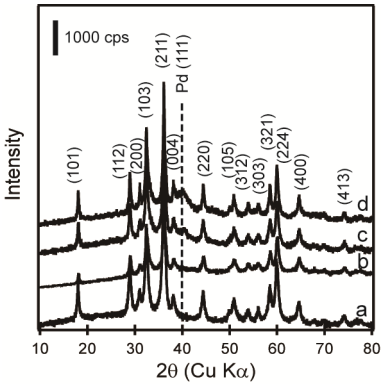

Figure 1. The XRD patterns of Mn_3O_4 support (a) and Pd/Mn_3O_4 catalysts with different Pd loading contents: 1.1 wt% (b), 2.7 wt% (c), 3.2 wt% (d).

The crystalline structures of these materials were first characterized by X-ray diffraction (XRD) analysis. Figure 1 depicts the XRD pattern of the obtained mesoporous Mn_3O_4. There is not any diffraction peaks in the small angle range indicating the disordered pore arrangement. However, a series of sharp and symmetrical Bragg diffraction peaks can be found in wide angle area, which demonstrates the well crystallized feature. All the peaks in the pattern can be well assigned as the characteristic reflection planes of tetragonal Mn_3O_4. No additional peaks from impurity can be found. Besides, the lattice constants, a = 5.753 Å and c = 9.436 Å, are also in agreement well with those of bulk Mn_3O_4 (PDF card no. 80-0382). When loaded with Pd, a peak emerged at 2θ = 40° which can be identified as (111) diffraction bands of face-centered cubic structure palladium (PDF card no. 65-6174). The diffraction intensity increases with the increase of Pd loading content. It should be noted that all the characteristic peaks of metallic Pd were broadened and weak indicating the highly dispersed amorphous or small palladium nanoparticles. However, due to the partial overlapping between diffraction peaks of Pd (111) and Mn_3O_4 (004), it is difficult to estimate the palladium particle size using the Scherrer equation.

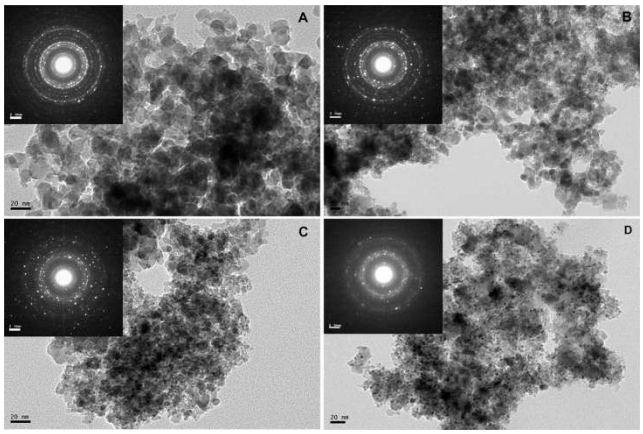

Figure 2. TEM images of Mn_3O_4 support (A) and Pd/Mn_3O_4 catalysts with different Pd loading contents: 1.1 wt% (B), 2.7 wt% (C) 3.2 wt% (D).

To get the details of the morphology and Pd distribution, the materials were examined with Transmission Electron microscopy (TEM). Figure 2 shows the TEM results of the mesostructured Mn_3O_4 support and Pd-loaded catalysts. For Pd-loaded catalysts, the Pd particles cannot be distinguished in the images, suggesting that the noble metal species have been highly dispersed into or on the mesoporous Mn_3O_4 support. The Selected-area-electron diffraction (SAED) patterns from the same area are also presented in the images. The well-defined diffraction rings for Mn_3O_4 can be found in all the samples. The relatively faint and disintegrated diffraction ring indicates its very low crystallinity and/or small size, which consists well with the above XRD results. The further High Resolution Transmission Electron microscopy (HRTEM) investigation clearly shows that the catalysts are composed of crystallized Mn_3O_4 and poorly crystallized Pd nanoparticles (Supporting information). Nanocrystals with different lattice d-spacing values can be found all over the image. Except for those with the d-spacing 2.2 Å assignable to Pd crystallite, all of them can be identified as Mn_3O_4 nanoparticles. The average size of Mn_3O_4, collected from over 10 different particles, was calculated to be 18 nm. Meanwhile, the highly dispersed Pd nanoparticles on the Mn_3O_4 support were mostly smaller than 10 nm. The template-assisted pyrolysis and impregnation method has been proved to be effective in fabricating noble metal-loaded Mn_3O_4 composite catalysts with noble metal nanoparticles homogeneously deposited into/on the polycrystalline Mn_3O_4 support.

The porous structure of the samples was further investigated by measuring adsorption-desorption isotherms of nitrogen at 77 K, as shown in Figure 3. In all the cases, the typical Langmuir IV

isotherms with H3 hysteresis loops indicate their porous structure and the formation of slit-like mesopores. The mesoporous structure of the Mn_3O_4 support has not changed even after impregnation and reduction treatment. However, different from other loading processes reported, their specific surface areas increase after the loading of palladium. Meanwhile, the pore size and pore volume of the Pd/Mn_3O_4 samples do not change significantly at increased Pd loading amounts (Supporting information). These results demonstrate that palladium nanoparticles have been highly dispersed into the pore channels and/or on the surface of the support, which is important to allow reactant molecules to diffuse into the mesostructure and access the catalytic nanoparticles.

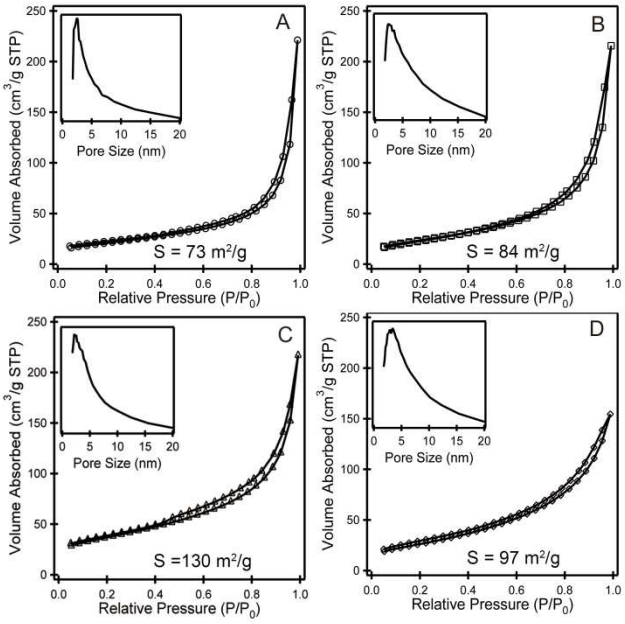

Figure 3. The N_2 adsorption-desorption isotherms of Mn_3O_4 support (A) and Pd/Mn_3O_4 catalysts with different Pd loading contents: 1.1 wt% (B), 2.7 wt% (C), 3.2 wt% (D).

X-ray photoelectron spectroscopy analysis (XPS) was used to determine surface chemical states of the species for meso-structured Mn_3O_4 and its Pd-loaded catalysts, as shown in Figure 4. For all the samples, there are two binding energy positions observed for Mn $2p_{3/2}$ (642.4 eV) and Mn $2p_{1/2}$ (654.0 eV) (Figure 4A). The detailed resolution of Mn $2p_{3/2}$ spectrum could produce three characteristic peaks at about 640.2 eV, 641.5 eV and 643.5 eV, corresponding to Mn^{2+}, Mn^{3+} and Mn^{4+}, respectively. [25, 26] From the calculated contents of different manganese species (Supporting information), it clearly indicates the surface manganese are mainly Mn^{3+} and Mn^{4+} and the content of Mn^{2+} species is as low as about 1%. This may due to the partial oxidation of surface manganese species when exposed to the air. The O 1s spectra recorded from these support and catalysts are also shown in Figure 4B. By means of deconvolution, the distribution of oxygen species was estimated and depicted. There are two kinds of oxygen species, the one at 530.4 eV is typical of metal-oxygen bonding, and the other at 531.5 eV and 532.3 eV is usually associated with the surface adsorbed oxygen. [27] With the

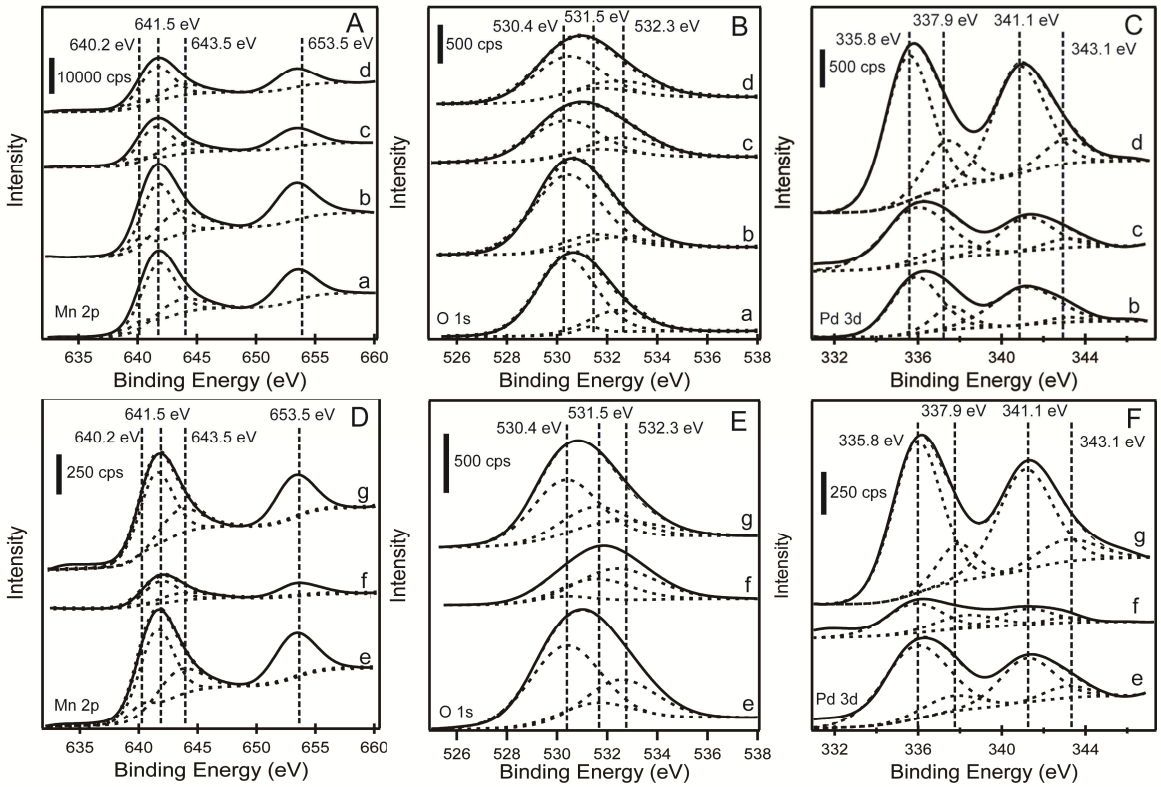

Figure 4. (A-C) The XPS spectra of Mn_3O_4 support (a) and Pd/Mn_3O_4 catalysts with different Pd loading contents: 1.1 wt% (b), 2.7 wt% (c), 3.2 wt% (d), (D-F) The XPS spectra of 2.7 wt% Pd loaded Pd/Mn_3O_4 catalyst before (e) and after reaction under dry condition (f), after reaction under moisture condition (g).

increase of Pd loading amount, the content of lattice O decreases, which may attributed to the highly dispersed Pd nanoparticles on the Mn_3O_4 surface. Typically, Pd^0 adsorptions are at 335.0 and 340.3 eV are for $3d_{5/2}$ and $3d_{3/2}$, respectively, with a spin-orbit separation of 4.7 eV. In three Pd/Mn_3O_4 samples, Pd $3d_{5/2}$ and $3d_{3/2}$ absorption peaks are all at slightly higher energy than that of Pd^0, implying the existence of small amount of positively charged Pd. After curve fitting, the calculated contents of Pd^0 and Pd^{2+} are about 90% and 10%, respectively. This clearly confirms that most of the Pd^{2+} ions in the surface have been reduced to Pd^0 by hydrazine hydrate.

Table 1. The surface atomic ratios determined by quantitative XPS analysis for 2.7 wt% Pd loaded catalyst before and after reaction.

Phase	Binding Energy (eV)	Fresh catalyst (%)	After reaction[c] (%)	After reaction[d] (%)
Mn^{2+}	640.2	0.2	6.4	1.1
Mn^{3+}	641.5	77.2	63.7	70.1
Mn^{4+}	643.5	22.6	27.8	28.8
Pd^0	335. 8 341.1	90.1	71.4	82.2
Pd^{2+}	337.9 343.1	9.9	28.6	17.8
O_{latt} [a]	530.4	57.5	8.9	54.9
O_{ads} [b]	531.5 532.3	42.5	91.1	45.1

[a] the lattice oxygen, [b] the oxygen absorbed on the surface of the catalyst, [c] after reaction under dry condition, [d] after reaction under moisture condition.

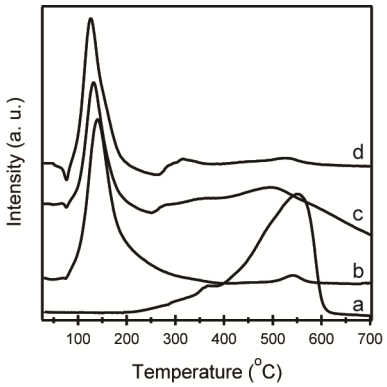

Figure 5. The H_2-TPR profiles of Mn_3O_4 support (a) and Pd/Mn_3O_4 catalysts with different Pd loading contents: 1.1 wt% (b), 2.7 wt% (c), 3.2 wt% (d).

H_2-Temperature-Programed Reduction (H_2-TPR) experiments were carried out to investigate the redox properties of various Mn_3O_4 supported palladium catalysts. Figure 5 shows the reduction profiles of the catalysts, and for comparison, the TPR profile of the parent Mn_3O_4 is also included. It has been well documented that the manganese oxides could be reduced between 300 °C and 600 °C. Not surprisingly, the mesoporous Mn_3O_4 support exhibits two reduction peaks, one at 380 °C and the other at 550 °C, indicating the stepwise reduction of manganese. [28-30] According to the literatures, the lower temperature peak may be roughly attributed to the reduction of Mn^{4+} to Mn^{3+}, whereas the higher one can be assigned as the consecutive reduction of Mn^{3+} to Mn^{2+}. This result corresponds well with the above XPS analysis. When incorporated with palladium two reduction peaks shift to lower temperatures, and such a shift is related with spill over effect involving either hydrogen activated on the metal phase or mobile lattice oxygen induced by intimate metal-support interactions. [7] The significant low-temperature reduction feature strongly suggests that the manganese oxide substrate has been 'activated' to a large extent in the Pd/Mn_3O_4 catalyst by Pd loading.

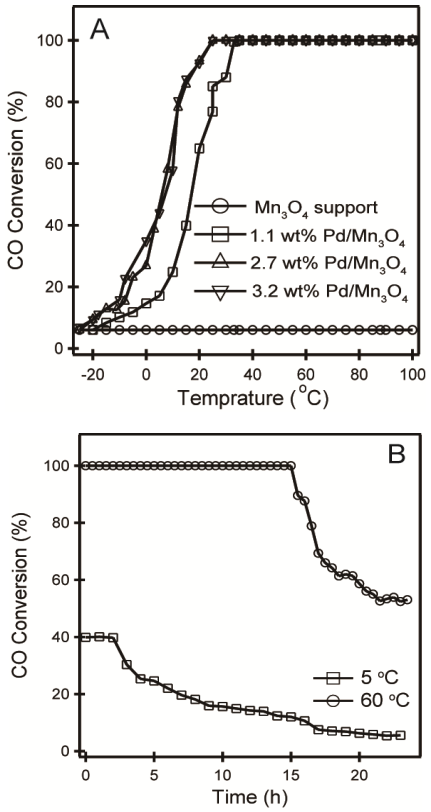

Figure 6. (A) The catalytic performances of Mn_3O_4 support and Pd/Mn_3O_4 catalysts with different Pd loading contents. (B) The stability of 2.7 wt% Pd loaded catalyst under dry condition at different temperatures.

The catalytic performances of mesoporous Mn_3O_4 and the corresponding mesostructured Pd loaded samples for CO oxidation are shown in Figure 6A, where the CO conversion is reported as a function of temperature. The mesoporous Mn_3O_4 support do not show any detectable catalytic activity when temperature lower than 100 °C. After incorporated with palladium, the activity for CO oxidation, as expected, is increased greatly which are notably higher than the Mn_3O_4 support. Under the same reaction condition, when the Pd loading content increases from 1.1 wt% to 2.7 wt%, the CO total conversion temperature accordingly decreases from 30 °C to 25 °C. However, further increasing the Pd content does not produce additional decrease of the conversion temperature. When the incorporated Pd content reaches to 3.2 wt%, the catalytic performance is almost the same as that of 2.7 wt%. This may be concerned with the size and distribution of the Pd nanoparticles in the catalysts, as shown in XRD analysis. Compared with other MnO_x supported Pd catalysts, all the samples exhibit excellent catalytic activity for CO oxidation. [31, 32]

Figure 4D-F also gives the surface chemical information for 2.7 wt% Pd loaded catalyst before and after CO oxidation. After CO oxidation reaction, there are variations in the valence states of Mn^{n+} and lattice oxygen, the amounts of Mn^{2+} and surface absorbed oxygen increase while those of Mn^{3+} and lattice oxygen

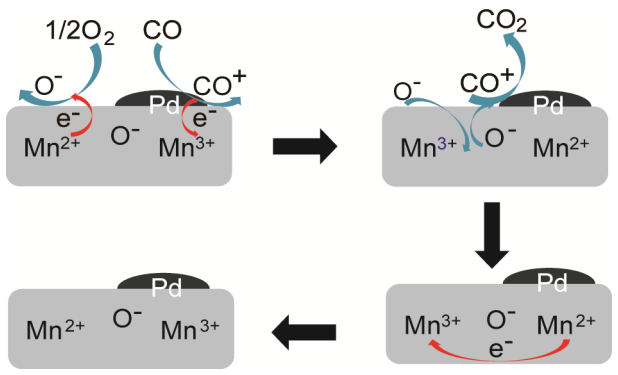

$Mn^{2+} \rightarrow Mn^{3+} + e^-$; $1/2\ O_2 + e^- \rightarrow O^-$;

$CO \rightarrow CO^+ + e^-$; $Mn^{3+} + e^- \rightarrow Mn^{2+}$;

$CO^+ + O^- \rightarrow CO_2$; $Mn^{2+} \rightarrow Mn^{3+} + e^-$; $Mn^{3+} + e^- \rightarrow Mn^{2+}$;

Scheme 1 The possible mechanism of Pd/Mn_3O_4 catalyst for CO oxidation reaction under dry condition.

decrease accordingly (Table 1). This phenomenon implies the take place of direct or indirect electron transfer processes among Mn^{n+} and participation of the lattice oxygen in the reaction during the CO oxidation process. Compared with other MnO_x supported Pd catalysts, Pd/Mn_3O_4 material showed much higher catalytic activities. [31, 32] Thus, the unique small amount of Mn^{2+} species of Mn_3O_4 support is considered to be a key factor for this excellent catalytic activity. The proposed synergetic catalytic effect on the catalytic oxidation of CO is illustrated in Scheme 1. In the proposed route, Pd particle adsorbs the CO molecule and captures one electron from it, and then delivers the electron to surface Mn^{3+} ion of the support, in the meantime, Mn^{3+} is reduced to Mn^{2+} and CO is activated into CO^+ species. The reaction between activated CO^+ species and lattice O leads to the quick formation of CO_2 on the interface between Pd and support leaving O vacant in the Mn_3O_4 structure. Meanwhile, Mn^{2+} of the support absorbs the O_2 molecular and donates an electron to the O atom, in the meantime, Mn^{2+} becomes Mn^{3+} and O_2 is turned to absorbed O^- species, which finally fill the O vacant in the support through diffusion. After electron transfer between Mn^{3+} and Mn^{2+}, Pd/Mn_3O_4 catalyst could recover its initial state.

It is worth to point out that the diffusion process of surface absorbed O^- ions to the lattice structure is always slower than that of absorption, ionization and reaction process. Thus, under the high CO concentration and given temperature, when the lattice oxygen on the interface was consumed completely, the conversion should be decreased until a new balance established between the consumption of the lattice O and diffusion of surface absorbed O^- to the lattice. Catalytic stabilities experiment under dry condition proved our above speculation (Figure 6B). At 5 °C, the catalytic activity of 2.7 wt% Pd loaded catalyst kept unchanged in the first 3 hours, sequential reaction caused gradual decrease of CO conversion. 16 hours later, when consumption of the lattice O equal to the diffusion of surface absorbed O^- to the lattice, CO conversion remained stable again. Similar result could also be formed in CO conversion curves at 60 °C.

Water is almost unavoidable in CO oxidation process especially in practical applications. It plays completely different role in the presence or absence of noble metal or transition metal oxide, which are the two most common types of catalysts for CO oxidation. On one hand, it can be a devastatingly poisonous species for transition metal oxide, the best example being the water-induced deactivation of Co_3O_4. On the other hand, a moderate amount of water on the surface of noble metals such as Au, Pt and Pd, can promote low-temperature CO oxidation due to the large amount of OH group induced by water molecules. A proposed mechanism indicates that formation of the COOH intermediate on the surface of noble metal is the key factor for H_2O assisted CO oxidation reaction. [7]

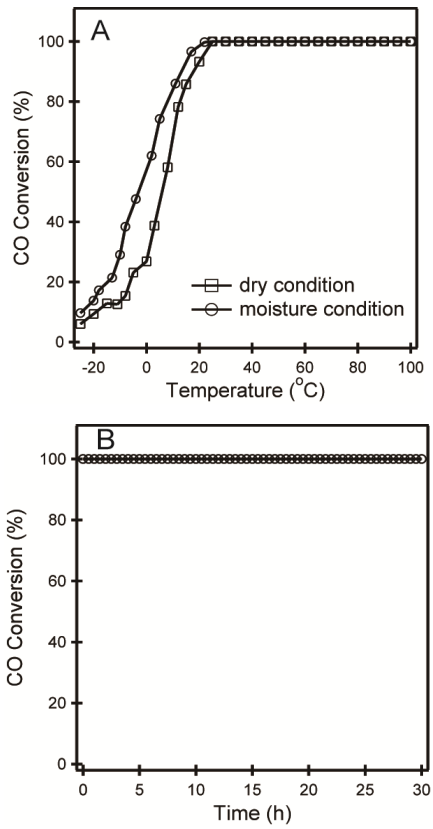

Figure 7. (A) The catalytic performances of 2.7 wt% Pd loaded catalyst under different conditions. (B) The catalytic stability of 2.7 wt% Pd loaded catalyst under moisture condition at 35 °C. (The water concentration in the feed gas is 4.0 vol%).

In Pd/Mn_3O_4 catalyst system, H_2O was found to be beneficial to the CO oxidation. The 2.7 wt% Pd loaded Mn_3O_4 catalyst was selected to test under moisture condition. The catalyst shows increased catalytic activities in CO oxidation compared with that under dry reaction condition (Figure 7A). The 100% conversion temperature decrease to 22 °C and that for 50% conversion (T_{50}) is as lower as 0 °C. Figure 7B depicts the catalytic stability for CO oxidation under moisture condition, no activity loss for CO conversion can be observed even after 30 hours of reaction, indicating the excellent stability of the composite catalyst under moisture condition. Based on above mechanism under dry condition and combined with XPS analysis results of the catalyst before and after reaction under moisture condition, the proposed synergetic effect mechanism is showed in Scheme 2.

Under the presence of moisture, H_2O directly participates in the CO oxidation reaction and lattice oxygen of the support

Mn_3O_4 does not. As there is no significant variation of the content of lattice O before and after reaction (Table 1), reaction mechanism under moisture condition can be proposed as follows.

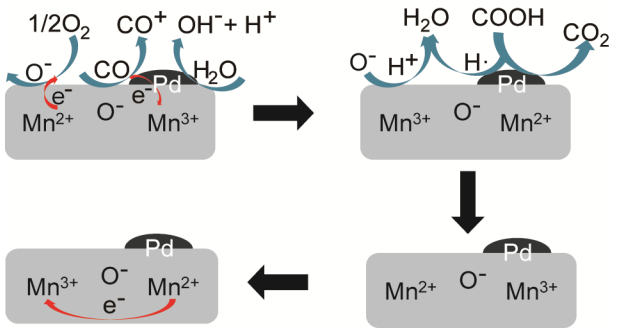

$Mn^{2+} \rightarrow Mn^{3+} + e^-$; $1/2\ O_2 + e^- \rightarrow O^-$;

$CO \rightarrow CO^+ + e^-$; $Mn^{3+} + e^- \rightarrow Mn^{2+}$; $H_2O \rightarrow OH^- + H^+$;

$CO^+ + OH^- \rightarrow COOH$; $COOH \rightarrow CO_2 + H\cdot$; $H\cdot + H^+ + O^- \rightarrow H_2O$;

$Mn^{2+} \rightarrow Mn^{3+} + e^-$; $Mn^{3+} + e^- \rightarrow Mn^{2+}$;

Scheme 2 The possible mechanism of Pd/Mn_3O_4 catalyst for CO oxidation reaction under moisture condition.

The Pd activated CO^+ species reacted with OH^- to form very reactive adsorbed intermediate, COOH, and then decomposed to CO_2 and H·. On the other hand, the O^- species supplied by Mn_3O_4 support absorbed O_2 molecular combined with H· and H^+ to form H_2O. In this mechanism, the CO_2 formation reaction only occurred on the surface of palladium, which avoid the contact between CO_2 and transition metal oxide and further prevent the formation of carbonates. Therefore, in spite of the existence of H_2O, the catalytic activity could keep stable during the CO oxidation process.

Conclusions

Mesostructured Mn_3O_4 supported Pd catalyst has been successfully fabricated through a facile template-assisted pyrolysis and impregnation strategy. The resulting materials possessed relatively high surface area and highly dispersed palladium species, and showed high catalytic activities for CO oxidation especially under moisture condition. For 2.7 wt% Pd loaded catalyst, the 100% conversion temperature was about 22 °C and that for 50% conversion was as lower as 0 °C. More important, the material showed excellent stability under moisture condition. The catalytic activity had not any decrease for CO conversion even after 30 hours reaction. This unique catalytic durability can be assigned to the synergetic effect between Pd nanoparticles and Mn_3O_4 support. The existence of small amount of surface Mn^{2+} species may be the key factor for this excellent catalytic activity.

Notes and references

[a] *Key Laboratory for Ultrafine Materials of Ministry of Education, School of Materials Science and Engineering, East China University of Science and Technology, Shanghai, 200237, China. Fax: +86-021-64250740; Tel: +86-021-64252599; E-mail: liliang@ecust.edu.cn*

[b] *State Key Laboratory of High Performance Ceramic and Superfine Microstructure, Shanghai Institute of Ceramics, Chinese Academy of Science, Shanghai 200050, China. E-mail: jlshi@sunm.shcnc.ac.cn*

† Electronic Supplementary Information (ESI) available: [details of any supplementary information available should be included here]. See DOI: 10.1039/b000000x/ This study was supported by National Basic Research Program of China (No. 2013CB933201).

1 M. Haruta, N. Yamada, T. Kobayashi, S. Iijima, *J. Catal.,* 2010, **115**, 301.
2 M. S. Chen, D. W. Goodman, *Science,* 2004, **306**, 252.
3 C. T. Campbell, *Science,* 2004, **306**, 234.
4 A. U. Nilekar, S. Alayoglu, B. Eichhorn, M. Mavrikakis, *J. Am. Chem. Soc.,* 2010, **132**, 7418.
5 A. Hadi, II. Yaacob, *Catal. Today,* 2004, **96**, 165.
6 J. Huang, S. Wang, Y. Zhao, X. Wang, S. Wang, S. Wu, S. Zhang, W. Huang, *Catal. Commun.,* 2006, **7**, 1029-1034.
7 J. Bergeld, B. Kasemo, D. V. Chakarov, *Surf. Sci.,* 2001, **495**, L815.
8 H.-F. Wang, R. Kavanagh, Y.-L. Guo, Y. Guo, G.-Z. Lu, P. Hu, *Angew. Chem. Int. Ed.,* 2012, **51**, 6657.
9 X. Xie, L. Li, Z.-Q. Liu, M. Haruta, W. J. Shen, *Nature,* 2009, **458**, 746.
10 M. Date, M. Okumura, S. Tsubota, M. Haruta, *Angew. Chem. Int. Ed.,* 2004, **43**, 2129.
11 M. Haruta, N. Yamada, T. Kobayashi, S. Iijima, *J. Catal.,* 1989, **115**, 301.
12 L.-C. Wang, Q. Liu, X.-S. Huang, Y.-M. Liu, Y. Cao, K.-N. Fan, *Appl. Catal. B,* 2009, **88**, 204.
13 H. G. Zhu, Z. Ma, J. C. Clark, Z. W. Pan, S. H. Overbury, S. Dai, *Appl. Catal. A,* 2007, **326**, 89.
14 W. S. Lee, B. Z. Wan, C. N. Kuo, W. C. Lee, S. F. Cheng, *Catal. Commun.,* 2007, **8**, 1604.
15 I. D. Gomez, I. Kocemba, J. M. Rynkowski, *Appl. Catal. B,* 2009, **88**, 83.
16 J. M. C. Soares, M. Hall, M. Cristofolini, M. Bowker, *Catal. Lett.,* 2006, **109**, 103.
17 L. Liu, F. Zhou, L. Wang, X. Qi, F. Shi, Y. Deng, *J. Catal.,* 2010, **274,** 1.
18 H. Zhu, Z. Qin, W. Shan, W. Shen, J. Wang, *J. Catal.,* 2004, **225**, 267.
19 J.-Y. Luo, M. Meng, X. Li, X.-G. Li, Y.-Q. Zha, T.-D. Hu, Y.-N. Xie, J. Zhang, *J. Catal.,* 2008, **254**, 310.
20 T. Jin, T. Okuhara, G. J. Mains, J. M. White, *J. Phys. Chem.,* 1987, **91**, 3310.
21 G. S. Zafiris, R. J. Gorte, *J. Catal.,* 1993, **139**, 561.
22 H. Cordatos, R. J. Gorte, *J. Catal.,* 1996, **159**, 112.
23 A. Tomcrona, M. Skoglundh, P. Thormahlen, E. Fridell, E. Jobson, *Appl. Catal. B,* 1997, **14**, 131.
24 A. Martinez-Arias, M. Fernandez-Garcia, A. Iglesias-Juez, A. B. Hungria, J. A. Anderson, J. C. Conesa, J. Soria, *Appl. Catal. B,* 2001, **31**, 39.
25 G. S. Qi, R. T. Yang, *J. Phys. Chem. B,* 2004, **108**, 15738.
26 Z. H. Chen,; F. R. Wang, H. Li, Q. Yang, L. F. Wang, X. H. Li, *Ind. Eng. Chem. Res.,* 2012, **51**, 202.
27 F. Morales, D. Grandjean, A. Mens, F. M. F. de Groot, B. M. Weckhuysen, *J. Phys. Chem. B,* 2006,**110**, 8626.
28 L. E. Gómez, E. E. Miró, A. V. Boix, *Int. J. Hydrogen Energy,* 2013, **38**, 5645.
29 K. Jirá tová, J. Mikulová, J. Klempa, T. Grygar, Z. Bastl, F. Kovanda, *Appl. Catal. A,* 2009, **361**, 106.
30 E. R. Stobbe, B. A. de Boer, J. W. Geus, *Catal. Today,* 1999, **47**, 161.
31 J. S. Park, D. S. Doh, K. Y. Lee, *Top. Catal.,* 2000, **10**, 127.
32 A. V. Salker, R. K. Kunkalekar, *Catal. Commun.,* 2009, **10**, 1776.

Table of content

The as synthesized Pd/Mn_3O_4 catalysts possess relatively high surface area and highly dispersed palladium species, and show much higher catalytic activity and stability for CO oxidation especially under moisture condition.